FEBS Letters 587 (2013) 504–509

FEBS Letters

journal homepage: www.FEBSLetters.org

Negative control of cell size in the cyanobacterium *Synechococcus elongatus* PCC 7942 by the essential response regulator RpaB

Félix Moronta-Barrios [1], Javier Espinosa [1], Asunción Contreras *

División de Genética, Universidad de Alicante, Apartado 99, E-03080 Alicante, Spain

ARTICLE INFO

Article history:
Received 18 December 2012
Revised 7 January 2013
Accepted 8 January 2013
Available online 20 January 2013

Edited by Richard Cogdell

Keywords:
Response regulator
Cyanobacteria
Essential two-component system
Cell size
RpaB

ABSTRACT

The essential NblS–RpaB pathway for photosynthesis regulation and acclimatization to a variety of environmental conditions is the most conserved two-component system in cyanobacteria. To get insights into the RpaB implication in cell homeostasis we investigated the phenotypic impact of altering expression of the essential *rpaB* gene of *Synechococcus elongatus* PCC 7942 and determined the in vivo levels of the RpaB and RpaB∼P polypeptides. Our results implicate non-phosphorylated RpaB in controlling cell length and shape and suggest that intrinsic regulation may be important to prevent drastic variations in RpaB levels and activity.

1. Introduction

Cyanobacteria, phototrophic organisms that perform oxygenic photosynthesis using light as energy source, have colonized a vast number of habitats. Not surprisingly, they contain more genes encoding two-component systems (TCSs) per unit genome size than other bacteria [1]. A high proportion of the response regulators (RRs) are orphan proteins that outnumber histidine kinases (HKs) by almost 2:1 (24:13 in the model system *Synechococcus elongatus* PCC 7942, hereafter referred to as *S. elongatus*). Amongst cyanobacterial RRs, the OmpR/PhoB family is predominant [2]. The most conserved TCS in cyanobacteria is formed by the HK NblS and the OmpR/PhoB RR RpaB.

A particularly large number of genes are controlled by NblS and RpaB under a variety of stress conditions [3,4] and plays a role in the transcriptional oscillation of clock-regulated genes [5]. RpaB binds to HLR1 sequences (High Light Regulatory 1) to regulate target genes [6]. We recently showed that the phosphorylated form of RpaB is present in *S. elongatus* cells growing under standard laboratory conditions and that high light stress affected the in vivo ratio of phosphorylated to non-phosphorylated RpaB [7].

NblS, RpaB and, importantly, key residues required for phosphorylation of these proteins are all essential for cell viability in the obligated photoautotroph *S. elongatus* [8], suggesting that the phosphorylated form of RpaB mediates functions that are required for growth during standard culture conditions. In *S. elongatus* and related cyanobacteria NblS, RpaB, and its non-essential paralog SrrA constitute a branched pathway. SrrA is preferentially phosphorylated by NblS in vitro but environmental repression of *srrA* prevents deleterious interference with the essential RpaB pathway [8]. SipA, a non-essential factor with a SH3 fold binds to the ATP binding domain (HATPase_c) of NblS and stimulates its auto-phosphorylation activity [9–11] in response to yet unknown signals.

Due to the essentiality of the NblS-RpaB pathway, the function of this system in cellular regulation is poorly understood, and thus it is important to develop approaches allowing informative manipulation of the genes. To get insights into the role of RpaB in survival and cell homeostasis under standard laboratory conditions, we constructed stable *S. elongatus* strains with either constitutively increased or decreased expression of the *rpaB* gene. The relatively small deviations of the intracellular RpaB levels achieved in this way were nevertheless large enough to reveal an inverse correlation between RpaB levels and cell length, subsequently confirmed with an IPTG-inducible RpaB overexpression strain. Our results argue in favor of a connection between RpaB and cell growth support the idea that both phosphorylated and non-phosphorylated RpaB perform specific roles under standard growth conditions and suggest that intrinsic regulation may be important to prevent an excess of RpaB activity.

* Corresponding author. Fax: +34 96 5909469.
E-mail address: contrera@ua.es (A. Contreras).
[1] These two authors contributed equally to this work.

0014-5793/$36.00
http://dx.doi.org/10.1016/j.febslet.2013.01.023

2. Materials and methods

2.1. Culture and growth conditions

S. elongatus strains were routinely grown photoautotrophically at 30 °C while shaking under constant illumination (30 μE m^{-2} s^{-1}) provided by cool white fluorescent lights. Photon flux densities were measured with Li-250 quantum-meter (Li-COR Bioscience). Media used was BG11 ($BG11_0$ plus 17.5 mM $NaNO_3$ and 10 mM HEPES/NaOH pH 7.8). Growth of cells in liquid cultures was measured by determining $OD_{750\ nm}$ in a UV/visible spectrophotometer Ultrospec 2100 *pro* (Amersham Biosciences). For growth on plates, the medium was solidified by addition of 1% (w/v) agar. Plates were incubated at 30 °C under constant illumination. *S. elongatus* strains were transformed as described by [12], incubated for 48 h at 30 °C under illumination on nitro-cellulose filters (Millipore), and transformants were selected on kanamycin or streptomycin-containing BG11 plates. Antibiotics concentrations used were 10 μg/ml (kanamycin) and 5 μg/ml (streptomycin). To overexpress RpaB, cultures were freshly diluted and IPTG added to final concentration of 1 mM.

2.2. Construction of plasmids and strains

All generated constructs were analyzed by automated dideoxy DNA sequencing. All cloning procedures were carried out in *Escherichia coli* DH5α using standard techniques. Strains and plasmids are listed in Table 1. Oligonucleotides are listed in Table S1.

To construct plasmid pUAGC758, a *Hinc*II fragment from pRL161 containing the C.K1 cassette was cloned into the *BstE*II site of Klenow-treated pUAGC589. To construct pUAGC763 and pUAGC764, *Eco*RV-*Hinc*II fragments from pUAGC453 containing the C.S3 cassette were cloned into the *BstE*II site of Klenow-treated pUAGC589. Transformation of *S. elongatus* with pUAGC758, pUAGC763 and pUAGC764 resulted in the CK1B, CS3B and CS3B(-) strains, respectively.

To construct pUAGC280, *lacI*^{q} and P*trc* sequences from pTrc99A were cloned into the *Sph*I and *Sal*I sites of pUAGC815. To construct pUAGC282 (encoding RpaB with four extra amino acids at the N-terminus), genomic *rpaB* sequences were PCR amplified with RpaB-PTRC-1F and RpaB-HCN-1R and cloned into the *Eco*RI and *Bam*HI sites of pUAGC280. Transformation of *S. elongatus* with pUAGC280 and pUAGC282 resulted in 1Ptrc and 1Ptrc-rpaB strains, respectively.

Table 1
Strains and plasmids.

Strain or plasmid	Genotype or relevant characteristics	Reference
E. coli DH5α	F$^-$ ϕ80d*lacZ*ΔM15Δ(*lacZYA-argF*)U169 *endA1 recA1*	
	hsdR17(r_K^- m_K^+) *deoR thi-1 supE44 gyrA96 relA1* λ$^-$	[22]
S. elongatus WT	Wild-type *S. elongatus* PCC 7942	Pasteur culture collection
S. elongatus CS3B	Φ(C.S3(+)–rpaB), Sm^r	This work
S. elongatus CK1B	Φ(C.K1(+)–rpaB), Km^r	This work
S. elongatus 1Ptrc	(P*trc*) NSI, Sm^r	This work
S. elongatus 1Ptrc-rpaB	Φ(P*trc*::*rpaB*) NSI, Sm^r	This work
pRL161	C.K1, Ap^r Km^r	[23]
pUAGC453	pBluescriptII SK(+) with C.S3, Ap^r Sm^r	[24]
pUAGC589	pBluescriptII SK(+) with a 1553 bp genomic *rpaB* fragment, Ap^r	[7]
pUAGC763	pUAGC589 with Φ(C.S3(+)-rpaB), Ap^r Sm^r	This work
pUAGC764	pUAGC589 with Φ(C.S3(−)-rpaB), Ap^r Sm^r	This work
pUAGC758	pUAGC589 with Φ(C.K1(+)-rpaB), Ap^r Sm^r	This work
pUAGC815	C.S3 into NSI, Ap^r Sm^r	[6]
pTrc99A	*E. coli* expression vector, source of *trc* promoter, Ap^r	Pharmacia biotech
pUAGC280	pUAGC815 derivative with *lacI*^{q} and P*trc*, Ap^r Sm^r	This work
pUAGC282	pUAGC280 with P*trc-rpaB*, Ap^r Sm^r	This work

2.3. Immunodetection methods and Phos-tag acrylamide SDS–PAGE separation of phosphorylated and unphosphorylated RpaB proteins

For protein extract preparation, *S. elongatus* cells were quickly harvested by centrifugation and the pellet resuspended in 100 μL of lysis buffer: 25 mM Tris–HCl pH 8.0, 1 mM DTT, Protease inhibitor cocktail (23 mM AEBSF, 2 mM Aprotinin, 130 μM Bestatin, 100 mM EDTA, 0.3 mM E-64, 0.3 mM Pepstatin A) and PhosSTOP (Roche). Glass beads were added and the mixture homogenized with three cycles of 1 min with a Minibeadbeater, under refrigeration. After centrifugation (5000×*g* 3 min 4 °C), the supernatant was recovered and protein content determined according to Lowry (Bio-Rad RC DC). RpaB inmunodetection and Phos-tag SDS–PAGE in combination with Western blot was carried exactly as described [7]. Band quantification was carried out by densitometry analysis of images with Image Quant TL (Amersham Biosciences). Negligible loss of RpaB phosphorylation resulted after protein extract preparation according to experiments with recombinant RpaB phosphorylated with acetyl-phosphate (data not shown).

2.4. Real-time RT-PCR

50 ml aliquots of exponentially growing *S. elongatus* cells ($OD_{750\ nm}$ 0.5) were used for RNA extractions, cDNA synthesis and quantitative PCR as described [7]. Primers for cDNA synthesis (RpaB7942–2R and RnpB-R for *rpaB* and *rnpB*, respectively) and qPCR (RpaB-QPCR-1F/RpaB7942–2R and RnpB-F/RnpB-R) are described in Supplementary Table S1. The assay consisted of two experiments with each sample in triplicate. The C_t difference between *rpaB* gene and endogenous control (*rnpB*) was ΔC_t. The difference between ΔC_t of mutants and WT was $\Delta\Delta C_t$. The cDNA *n*-fold change for each gene at selected strains was determined according to $2^{-\Delta\Delta C_t}$.

2.5. Microscopy, image acquisition and analysis

Exponentially growing cells were mounted on 1% low-melting point agarose pads for microscopy. Visualization of auto fluorescence signal and image analysis was as described [7]. Images (8-bit, 1024 × 1024 pixels) were recorded at 200 Hz, averaging each line eight times. All images were captured with all pixels below saturation and analyzed with ImageJ software [13]. To obtain cell length and width parameters the auto fluorescent signal from the thylakoids was used as a reference for cell edges (Supplementary Fig. S1 and Table S2 for details). 50 non-dividing cells (without middle constriction) were measured for each strain or condition.

3. Results

3.1. Up and down mutations at the rpaB locus of S. elongatus. Effect on transcript and protein levels

To investigate the in vivo function and regulation of RpaB in genetically stable backgrounds, we constructed *S. elongatus* strains with insertions altering the levels of expression of the *rpaB* gene. To decrease *rpaB* expression, the streptomycin-resistant cassette C.S3 was introduced, in each of the two possible orientations, between the *rpaB* promoter and the upstream HLR1 box. In parallel, a construct was designed to increase *rpaB* expression by taking

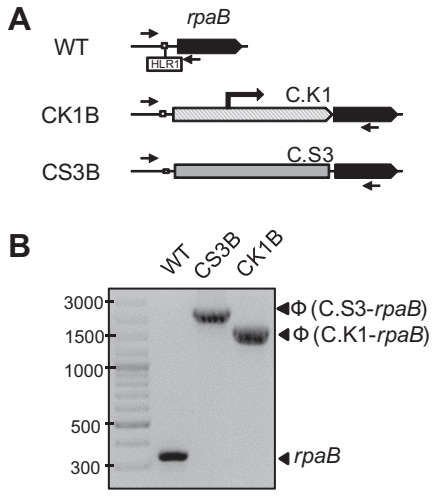

Fig. 1. Insertion of C.K1 and C.S3 cassettes upstream *rpaB*. (A) Schematic representation of the *rpaB* chromosomal region and position of the HLR1 box in the indicated strains. The strong promoter in C.K1 is represented as a thick black arrow. Black arrows signal the position of PCR primers. (B) PCR analysis of representative clones with indication of the amplified alleles and reference size bands from the marker (GeneRuler 100 bp leader, Fermentas).

advantage of the strong promoter from the C.K1 cassette, which was inserted in exactly the same position chosen for the C.S3 insertion. After independent transformation of *S. elongatus* with each of the three constructs, subsequent culture of streptomycin- and kanamycin-resistant clones resulted in the CS3B(+), CS3B(−) and CK1B strains carrying, respectively, completely segregated Φ(C.S3(+)-*rpaB*), Φ(C.S3(−)-*rpaB*) and Φ(C.K1-*rpaB*) alleles, confirming the viability of both types of insertions at the *rpaB* upstream region. Details of strain construction and representative PCR analysis to verify segregation are shown in Fig. 1. Since strains CS3B(+) and CS3B(−) were indistinguishable in our assays, for simplicity only data from strain CS3B(+), abbreviated to CS3B, is represented hereafter.

To ascertain the impact of the introduced cassettes on gene expression, we determined *rpaB* transcript levels in CS3B, CK1B and the wild type strains by quantitative RT-PCR. Both insertions resulted in significant alterations of the *rpaB* transcript levels found in the control strain, consistent with slightly down- and strongly up-regulation of *rpaB* transcript levels in CS3B (0.355 ± 0.045) and CK1B (15.45 ± 0.75), respectively. Thus, a 42-fold difference in transcript levels was found between CS3B and CK1B strains.

Protein extracts from the three strains were subsequently subjected to Western blotting with anti-RpaB antibody and the RpaB levels were quantified relative to those of the wild type control (Fig. 2A). The corresponding values for CS3B (0.55 ± 0.02) and CK1B (2.94 ± 0.26) indicated that the impact of the insertion mutations on protein levels was less pronounced than on transcripts levels, and this was particularly true in the case of CK1B. Therefore, differences in protein levels between CS3B and CK1B strains amounted to just 5.3-fold.

3.2. Effect of RpaB levels in S. elongatus cell size and culture growth

As part of the initial characterization of the CS3B and CK1B strains, cells from exponentially growing cultures were observed by Laser Scanner Confocal Microscopy (LSCM). Although cells from the different cultures compared in the same conditions looked very much alike, we noticed that CS3B cells appeared on average longer than CK1B cells and, to a lesser extent, longer than the wild type control (Fig. 2B).

To further investigate the possible (inverse) correlation between cell length and RpaB protein levels, additional strains were constructed to test the prediction that increasing the intracellular RpaB levels beyond the levels found in strain CK1B would further reduce cell length (Fig. 3A and B). Strain 1Ptrc-rpaB carries a P*trc*::*rpaB* translational fusion (providing an AUG start to replace the UUG initiation codon of *rpaB*) and *lacI*^{q} into the Neutral Site I (hereafter NSI) of *S. elongatus*, allowing *rpaB* overexpression in an IPTG-inducible manner. In the absence of IPTG, 1Ptrc-rpaB and the control strain 1Ptrc contained similar RpaB levels and retained wild type morphology. However, IPTG treatment of 1Ptrc-rpaB, induced RpaB accumulation and resulted in shorter and wider cells that stopped growing, in contrast to the control strain 1Ptrc (Fig. 3C–E). Therefore, the results confirmed a decrease in cell size proportional to the RpaB levels, further revealing that changes in cell length are compensated with opposite changes in the cell diameter and that very high levels of RpaB prevent culture growth.

To quantitate the differences between strains, we measured each of the two dimensions, length and width, in representative populations of wild type and derivative strains. As shown in Table 2,

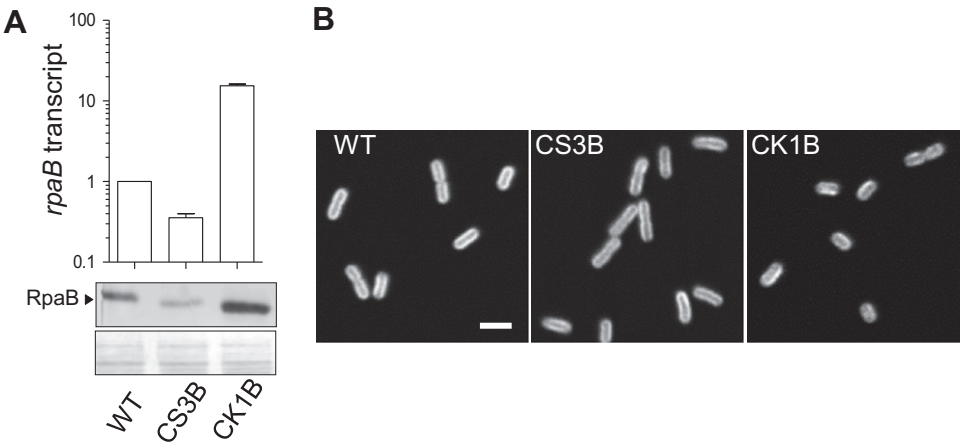

Fig. 2. Expression of *rpaB* and cell appearance in *S. elongatus* derivatives. (A) Top panel: quantitative RT-PCR for *rpaB* transcripts. Means and SEM values, from two independent experiments carried out in triplicate, normalized and relative to the WT levels are plotted. Middle panel: representative immunodetection of RpaB after SDS–PAGE. Quantification of the intensities of bands from four independent experiments gave values of 0.55 ± 0.02 for CS3B and of 2.94 ± 0.26 for CK1B relative to the WT (set arbitrarily to one). Protein loading and transfer quality is shown in bottom panel. (B) Auto fluorescence images of the same strains during exponential growth under standard conditions. Scale bar 2 μm (white bar).

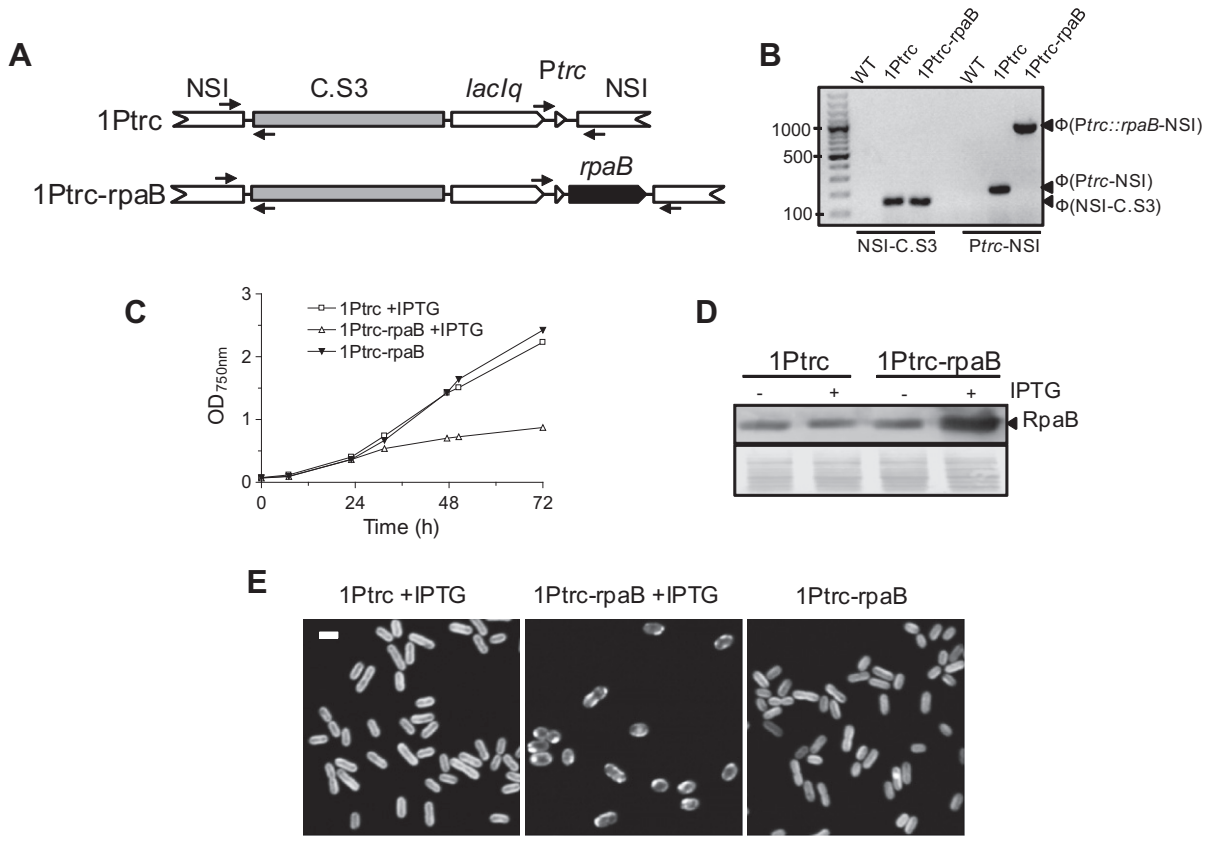

Fig. 3. Conditional overexpression of *rpaB*. (A) Schematic representation of the relevant chromosomal region of strains 1Ptrc and 1Ptrc-rpaB. (B) PCR amplification of the NSI-C.S3 and Ptrc-NSI frontiers from representative strain clones. (C) Effect of IPTG addition (1 mM) on growth of strains 1Ptrc and 1Ptrc-rpaB. (D) and (E) Representative immunodetection of RpaB and cell auto fluorescence, respectively, at 72 h after addition of IPTG. Other details as in Figs. 1 and 2.

significant differences were found in cell length between wild type and both CS3B and CK1B, and in cell width between wild type and CK1B, the ratio between length and width (*L*/*W*) being 2.25 in the wild type control, 3.06 in CS3B and 1.98 in CK1B. In addition, overexpression of RpaB in strain 1Ptrc-rpaB dramatically affected both length and width, reducing the *L*/*W* value to 1.53 under the tested conditions. The significance of these differences was assessed with a two-tailed Student *t*-test. *P* values for pairwise comparisons were <0.05 in all cases (Supplementary S3).

3.3. Both, increasing and decreasing RpaB levels have a negative impact on the levels of RpaB∼P in S. elongatus

Next, we investigated the possibility that altering the physiologically relevant levels of RpaB might change the in vivo equilibrium between RpaB phosphorylation and de-phosphorylation reactions. The levels of both RpaB∼P and RpaB polypeptides were determined from comparable extracts of wild type, CS3B, and CK1B cultures subjected to Phos-tag acrylamide electrophoresis and subsequent analyses by Western-blotting. The results, relative to the total amount of RpaB in the wild type strain, are represented in Fig. 4. The relative RpaB∼P and RpaB values were respectively, 0.38 and 0.62 in the wild type control, 0.16 and 0.34 in CS3B and 0.26 and 2.5 in CK1B, and thus the RpaB∼P/total RpaB ratio was 0.38 in the wild type control, slightly lower in CS3B (0.32) and much lower in CK1B (0.09).

3.4. Role of RpaB and RpaB∼P in S. elongatus cell shape

To integrate the results obtained from different analyses, we represented the *L*/*W* values against the levels of total RpaB, RpaB∼P and unphosphorylated RpaB for WT, CS3B and CK1B. Fig. 5 illustrates that the largest differences in cell shape (*L*/*W* value) amongst the three strains are found between CS3B (3.06) and CK1B (1.98) and that these strains also showed the largest differences in the amount of unphosphorylated (7.3 times) and total RpaB (5.5 times). In contrast, RpaB∼P levels changed very little between these two strains (1.6 times) and, importantly, the WT strain showed the highest RpaB∼P levels of the three, thus excluding the idea that the RpaB∼P levels have a main role in determining the cell shape.

4. Discussion

The cyanobacterial NblS-RpaB signaling pathway has already been the subject of multiple studies emphasizing its importance in acclimatization to stress, but genetic analysis of the pathway is complicated because null mutations, or even point mutations in the phosphorylatable residues, were not viable in *S. elongatus* [8]. In addition to the essentiality of *rpaB*, the stability of the RpaB protein levels [5,7,14] and the complexity of the regulatory interactions in which RpaB participates suggested to us that the *rpaB* gene dosage may be important for cell homeostasis. To test this idea we studied phenotypic consequences of mutations in *cis* affecting *rpaB* expression following a previously successful strategy based on introducing the C.K1 or C.S3 cassettes upstream of the target gene [15]. While C.K1 increases transcript levels by providing a strong outwards promoter, C.S3 may interfere with activation from the upstream HLR1 box, an element that may be involved in fine tuning *rpaB* gene expression [7].

Several observations suggest that in *S. elongatus*, posttranscriptional regulation prevent drastic and deleterious variations in the intracellular accumulation of RpaB. Total RpaB levels appear to

Table 2
Cell length and width of different *rpaB* derivative strains.

Strain	Length (μm)	Width (μm)	*L*/*W* ratio
WT	2512 ± 0035	1118 ± 0011	2257 ± 0036
CS3B	3089 ± 0051	1019 ± 0013	3066 ± 0072
CK1B	2128 ± 0034	1084 ± 0013	1983 ± 0045
1Ptrc	2513 ± 0058	1099 ± 0013	2302 ± 0057
1Ptrc-rpaB	2285 ± 0033	1498 ± 0017	1534 ± 0026

Mean values with SEM of cell length, width and *L*/*W* ratio corresponding to 50 cells of each strain (data in Table S2). 1Ptrc and 1Ptrc-rpaB data correspond to 72 h after IPTG addition.

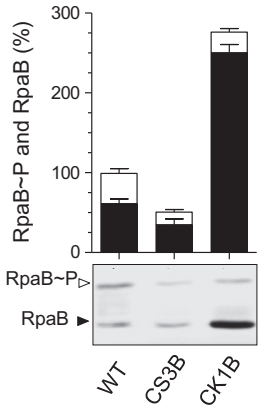

Fig. 4. RpaB and RpaB∼P polypeptides in *S. elongatus* derivatives. Top panel: the means and SEM of RpaB∼P (white bars) and RpaB (black bars) forms, determined from four independent Phos-tag experiments, are plotted. The total length of the bars indicate the total RpaB (RpaB + RpaB∼P) levels relative to that in wild type (set arbitrarily to 100). Values of RpaB and RpaB∼P for each strain were: 61.8 ± 6.1 and 38.2 ± 6.1 for WT, 34.5 ± 7.7 and 16 ± 3.4 for CS3B, 250 ± 10.7 and 26 ± 4.7 for CK1B. A representative Phos-tag experiment is shown below the stacked graph. The positions of RpaB∼P and RpaB are indicated as white and black arrowheads, respectively.

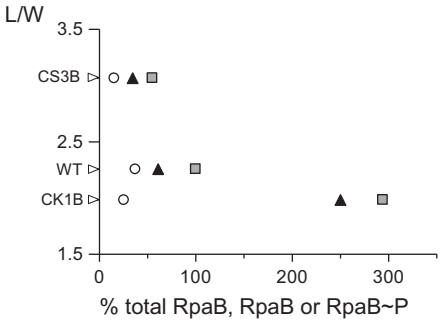

Fig. 5. Correlation between the *L*/*W* values (from Table 2) and the levels of RpaB (▲), RpaB∼P (○) or total RpaB (■) (from Fig. 4) for the indicated strains.

be constant under all tested conditions [5,7,14] and, although we observed up to a 42-fold difference in transcript levels between CS3B and CK1B strains, at the protein level the differences were significantly smaller: 5.3–5.5 differences depending on the type of immunodetection approach (Figs. 2 and 4). These relatively small variations in RpaB levels resulted in significant differences in cell size but not in culture growth rates. While the growth curves of wild type, CK1B and CS3B strains were identical (data not shown), overexpression of RpaB from a P*trc*::*rpaB* translational fusion lead to the cessation of growth (Fig. 3). Additional genetic work would be required to clarify the suggested roles of RpaB on the output pathway of the circadian clock [5] and cell division (this work).

The CK1B and CS3B strains provided an unexpected opportunity to compare healthy cultures of *S. elongatus* differing in the relative proportion of phosphorylated and unphosphorylated proteins. Strikingly, there was not a simple relationship between total RpaB and RpaB∼P levels when wild type and derivative strains were compared, suggesting a complex regulation of the RpaB∼P/RpaB ratio in *S. elongatus*. Regardless of the molecular basis of this finding, the prediction was that a cell function that would strictly depend on the wild type levels of RpaB∼P, which is thought to constitute the active form, would be impaired in strains with lower RpaB∼P levels (that includes CK1B and, to a greater extension, CS3B). Instead, we found a simple relationship between the length of *S. elongatus* cells, a complex trait for which the putative RpaB gene targets are yet unknown, and the levels of unphosphorylated (and total) RpaB polypeptides.

The existence of dual RRs having activity in both the phosphorylated and the unphosphorylated forms, have been inferred in other systems [16,17]. Our results, showing the importance of the levels of unphosphorylated RpaB for cell length, also argue against a simplistic on/off model for RpaB activity. Despite its essentiality in *S. elongatus*, preventing straightforward classical genetic approaches, the in vivo abundance of RpaB [7] and the relatively high stability of RpaB∼P [8] points to the RpaB system as a good model to gain insights into dual RRs.

The impact of relatively small variations of the RpaB protein levels on *S. elongatus* cell size suggests the involvement of the NblS-RpaB system in cell elongation. The almost spherical cell shape resulting from greater accumulation of RpaB is reminiscent of the phenotypes caused by mutations targeting the peptidoglycan sacculus and cytoskeleton proteins [18,19] or by overproducing the response regulator YycF [20]. In this context, we already noted similarities between the YycGF, WalKR and VicKR essential systems involved in cell-wall metabolism in Gram-positive bacteria [21] and the NblS-RpaB system [8]. Further work is required to reveal the identity of the RpaB targets involved in cell morphogenesis.

Acknowledgments

This work was supported by the Ministerio de Ciencia e Innovación (Grant BFU2009-07371) and the Generalitat Valenciana (ACOMP2911/211).

We are grateful to M.J. García-Sola for help with LSCM and to Drs. R. Dixon, F. Rodriguez-Mateos, and A. Marina for constructive discussions.

Appendix A. Supplementary data

Supplementary data associated with this article can be found, in the online version, at http://dx.doi.org/10.1016/j.febslet.2013.01.023.

References

[1] Ashby, M.K. and Houmard, J. (2006) Cyanobacterial two-component proteins: structure, diversity, distribution, and evolution. Microbiol. Mol. Biol. Rev. 70, 472–509.
[2] Galperin, M.Y. (2010) Diversity of structure and function of response regulator output domains. Curr. Opin. Microbiol. 13, 150–159.
[3] van Waasbergen, L.G., Dolganov, N. and Grossman, A.R. (2002) *nblS*, a gene involved in controlling photosynthesis-related gene expression during high light and nutrient stress in *Synechococcus elongatus* PCC 7942. J. Bacteriol. 184, 2481–2490.
[4] Tu, C.J., Shrager, J., Burnap, R.L., Postier, B.L. and Grossman, A.R. (2004) Consequences of a deletion in *dspA* on transcript accumulation in *Synechocystis* sp. strain PCC6803. J. Bacteriol. 186, 3889–3902.
[5] Hanaoka, M. et al. (2012) RpaB, another response regulator operating circadian clock-dependent transcriptional regulation in *Synechococcus elongatus* PCC 7942. J. Biol. Chem. 287, 26321–26327.

[6] Kappell, A.D. and van Waasbergen, L.G. (2007) The response regulator RpaB binds the high light regulatory 1 sequence upstream of the high-light-inducible *hliB* gene from the cyanobacterium *Synechocystis* PCC 6803. Arch. Microbiol. 187, 337–342.
[7] Moronta-Barrios, F., Espinosa, J. and Contreras, A. (2012) In vivo features of signal transduction by the essential response regulator RpaB from *Synechococcus elongatus* PCC 7942. Microbiology 158, 1229–1237.
[8] Lopez-Redondo, M.L., Moronta, F., Salinas, P., Espinosa, J., Cantos, R., Dixon, R., Marina, A. and Contreras, A. (2010) Environmental control of phosphorylation pathways in a branched two-component system. Mol. Microbiol. 78, 475–489.
[9] Espinosa, J., Fuentes, I., Burillo, S., Rodriguez-Mateos, F. and Contreras, A. (2006) SipA, a novel type of protein from *Synechococcus* sp. PCC 7942, binds to the kinase domain of NblS. FEBS Microbiol. Lett. 254, 41–47.
[10] Lopez-Redondo, M.L., Contreras, A., Marina, A. and Neira, J.L. (2010) The regulatory factor SipA is a highly stable beta-II class protein with a SH3 fold. FEBS Lett. 584, 989–994.
[11] Salinas, P., Ruiz, D., Cantos, R., Lopez-Redondo, M.L., Marina, A. and Contreras, A. (2007) The regulatory factor SipA provides a link between NblS and NblR signal transduction pathways in the cyanobacterium *Synechococcus* sp. PCC 7942. Mol. Microbiol. 66, 1607–1619.
[12] Golden, S.S. and Sherman, L.A. (1984) Optimal conditions for genetic transformation of the cyanobacterium *Anacystis nidulans* R2. J. Bacteriol. 158, 36–42.
[13] Schneider, C.A., Rasband, W.S. and Eliceiri, K.W. (2012) NIH Image to ImageJ: 25 years of image analysis. Nat. Methods 9, 671–675.
[14] Hanaoka, M. and Tanaka, K. (2008) Dynamics of RpaB-promoter interaction during high light stress, revealed by chromatin immunoprecipitation (ChIP) analysis in *Synechococcus elongatus* PCC 7942. Plant J. 56, 327–335.
[15] Espinosa, J., Castells, M.A., Laichoubi, K.B., Forchhammer, K. and Contreras, A. (2010) Effects of spontaneous mutations in PipX functions and regulatory complexes on the cyanobacterium *Synechococcus elongatus* strain PCC 7942. Microbiology 156, 1517–1526.
[16] Kobayashi, K. (2007) Gradual activation of the response regulator DegU controls serial expression of genes for flagellum formation and biofilm formation in *Bacillus subtilis*. Mol. Microbiol. 66, 395–409.
[17] Latasa, C. et al. (2012) *Salmonella* biofilm development depends on the phosphorylation status of RcsB. J. Bacteriol. 194, 3708–3722.
[18] Typas, A., Banzhaf, M., Gross, C.A. and Vollmer, W. (2012) From the regulation of peptidoglycan synthesis to bacterial growth and morphology. Nat. Rev. Microbiol. 10, 123–136.
[19] Vollmer, W. (2012) Bacterial growth does require peptidoglycan hydrolases. Mol. Microbiol. 86, 1031–1035.
[20] Fukuchi, K., Kasahara, Y., Asai, K., Kobayashi, K., Moriya, S. and Ogasawara, N. (2000) The essential two-component regulatory system encoded by *yycF* and *yycG* modulates expression of the *ftsAZ* operon in *Bacillus subtilis*. Microbiology 146, 1573–1583.
[21] Dubrac, S., Bisicchia, P., Devine, K.M. and Msadek, T. (2008) A matter of life and death: cell wall homeostasis and the WalKR (YycGF) essential signal transduction pathway. Mol. Microbiol. 70, 1307–1322.
[22] Hanahan, D. (2010) Techniques for transformation of *Escherichia coli* in: DNA Cloning (Glover, D.M., Ed.), pp. 109–135, IRL Press, Oxford, UK.
[23] Elhai, J. and Wolk, C.P. (1988) A versatile class of positive-selection vectors based on the nonviability of palindrome-containing plasmids that allows cloning into long polylinkers. Gene 68, 119–138.
[24] Ruiz, D., Salinas, P., Lopez-Redondo, M.L., Cayuela, M.L., Marina, A. and Contreras, A. (2008) Phosphorylation-independent activation of the atypical response regulator NblR. Microbiology 154, 3002–3015.